Received: 27 May 2022 | Revised: 6 September 2022 | Accepted: 18 October 2022

DOI: 10.1002/aic.17952

AIChE JOURNAL

RESEARCH ARTICLE

Reaction Engineering, Kinetics and Catalysis

Stationary states of hydrogen-producing reactions in nonequilibrium plasma

Xiaoshuang Chen | Elijah Thimsen

Department of Energy, Environmental and Chemical Engineering, Washington University in Saint Louis, Saint Louis, Missouri, USA

Correspondence
Elijah Thimsen, Department of Energy, Environmental and Chemical Engineering, Washington University in Saint Louis, Saint Louis, MO 63130, USA.
Email: elijah.thimsen@wustl.edu

Funding information
U. S. National Science Foundation, Grant/Award Number: CBET 1847469

Abstract

In this work, stationary states of hydrogen-producing reactions in nonequilibrium plasmas are explored, namely the water splitting and water gas shift reactions. For both reactions, the effluent from the reactor at long residence times in the plasma was found to be independent of the influent speciation. In other words, feeding the reactor either $0.1H_2O$ or $0.1H_2 + 0.05O_2$ by mole produced the same effluent composition, and similarly, feeding the reactor $0.1CO + 0.1H_2O$ produced nominally the same effluent as $0.1CO_2 + 0.1H_2$. For both reactions, the effluent from the plasma was found to be very far from local equilibrium at the total pressure and background temperature of the plasma and shifted in the endothermic direction relative to the local equilibrium speciation. This work further demonstrates that special attention must be paid to the recombination zone in plasmachemical processes. The recombination zone tends to drive the gas composition from plasma stationary states back towards local equilibrium.

KEYWORDS
irreversible thermodynamics, low-pressure reactor, low-temperature plasma, nonequilibrium thermodynamics, plasma chemistry, principle of maximum entropy production, superlocal equilibrium, water gas shift reaction, water splitting reaction

1 | INTRODUCTION

The thermodynamic concept of chemical reaction equilibrium is compelling because the terminal molecular speciation of a chemical system does not depend on the species fed into the reactor. Rather, it depends only on the temperature, pressure, and relative amounts of different elements in the system. That idea is encoded in the method of Gibbs minimization that can be used for calculating the mole fractions of different species at equilibrium,[1] which does not require explicit statement of any chemical reactions at all. The idea has important practical consequences. For example, gasification processes designed to generate synthesis gas ($CO + H_2$) can take complex feedstocks provided the process operates at an appropriate temperature and pressure (e.g., 1 bar and 1000°C), and the relative amounts of carbon, hydrogen, and oxygen atoms have specified values, for example, C:H:O = 1:2:1. This thermodynamic control achieved in systems with fast reaction kinetics allows approximately the same product ($CO + H_2$) to be synthesized from different feedstocks. For example, elemental carbon ($C + H_2O$), or polyethylene ($[CH_2]_x + x/2O_2$), or cellulose ($[C_6H_{10}O_5]_x + xH_2O$), would all produce the same equilibrium product distribution of nominally $CO + H_2$ at an appropriately high temperature. The phenomenon is the fundamental basis of chemical gasification process technology, which is a means of valorizing coal, waste plastics, and biomass. Recent research in gasification has focused on waste plastics, see for example, a review by Lopez et al.,[2] and co-gasification of multiple feedstocks, see for example, a recent review by Shahbaz et al.[3] Work also continues to understand the devolatilization process in the mature technology of coal gasification, for example, modeling changes in aliphatic structure[4] and heat transfer and volatile evolution inside coal particles.[5] At a fundamental level, to apply the idea of chemical reaction equilibrium, the system must be governed by

local equilibrium; and that is a good assumption for thermal systems driven for example, by the combustion of a fossil fuel.

A recent development is the plummeting cost of electricity produced from renewable sources such as photovoltaics,[6] and interest continues in fuels produced from those renewable sources.[7] For example, in the year 2010, the levelized cost of electricity produced by utility-scale photovoltaics was approximately 0.27 $/kWh. A decade later in the year 2020, the price had decreased to 0.046 $/kWh, and the Department of Energy goal is 0.02 $/kWh by 2030.[8] Electricity produced by renewable sources is already competitive with fossil fuels in many locations and may become generally less expensive. Electricity can, of course, be used as a source of heat to drive the same types of reactions that have been explored for years, such as gasification. However, electricity is a low entropy form of energy termed work, and for that reason, it is capable of promoting endergonic transformations that are not intrinsically constrained to proceed in the direction of local equilibrium at the background temperature and pressure of the reactor.[9]

Nonequilibrium plasma reactors are an example of an open-driven system that can utilize this low entropy feature of electricity.[9] Nonequilibrium plasmas are partially ionized gases. The minimum description of a nonequilibrium plasma is a system comprised of free electrons that have a very high temperature on the order of 10,000 K, immersed in a background gas comprised of heavy molecules and ions that typically have a temperature in the range from 300 to 1000 K.[9] Since the system is constrained by an external electricity flow to have multiple temperatures, it is a dissipative structure that is intrinsically very far from local equilibrium. Therefore, chemical reactions in nonequilibrium plasmas are not constrained to proceed towards the local equilibrium state at the background temperature of the heavy molecules and ions. More specifically, in recent experimental[10] and theoretical work,[11] our group has demonstrated that chemical reactions in nonequilibrium plasmas approach a stationary state that is in the nonlinear regime of irreversible thermodynamics. The result is important, because it means that the effluent from the reactor can have a higher free energy than the influent. In other words, if the influent is depleted, the reactor acts to reenergize the material to produce an effluent with higher chemical potential. For example, we have previously demonstrated CO_2 splitting into $CO + 1/2O_2$.[10] The influent was CO_2 and the effluent was mostly $CO + 1/2O_2$. The CO is reactive and useful, for example, it could be used to generate hydrogen by the water gas shift reaction. Interestingly, the same effluent composition was attained regardless of whether the initial speciation was pure CO_2 or $CO + 1/2O_2$ with the same overall elemental fractions.[10] In other words, the stationary state was independent of the initial speciation provided the plasma and overall elemental concentrations were held constant. The CO_2 splitting example illustrates the concept for a single chemical reaction involving only three species, but there is a question of whether the idea of chemical reactions in nonequilibrium plasma approaching stationary states is more broadly applicable to systems that involve multiple reactions and more chemical species. The answer to that question is critical to reaction engineering in nonequilibrium plasma processing of abundant natural resources such as water, biomass, and natural gas.

This work focuses on two chemical reactions that are important for energy applications because they can produce hydrogen. More specifically, the focus is on water splitting Reaction (R1) and water gas shift Reaction (R2). These reactions can be written as:

$$H_2O \rightarrow H_2 + 1/2O_2, \tag{R1}$$

$$CO + H_2O \rightarrow H_2 + CO_2. \tag{R2}$$

Reaction (R1) is highly endothermic as written, while Reaction (R2) is slightly exothermic. The basic approach is to measure the effluent composition from the reactor for different influent compositions, that is, H_2O or $H_2 + 1/2O_2$ for Reaction (R1); $CO + H_2O$ or $H_2 + CO_2$ for Reaction (R2). If at sufficiently long gas residence times, for constant plasma generation conditions, different influent compositions produce the same effluent composition, then a stationary state in the plasma has been reached. It is important to note that the observation of the effluent composition is made after it has passed through a recombination zone immediately after the plasma, and that recombination zone is governed by local equilibrium. See for example, an early report of the idea of a recombination zone in nonequilibrium plasmachemical reactors from Brown and Bell in the year 1974,[12] as well as a more recent description of the terminal state of the reaction in the recombination zone compared to the plasma zone.[11]

The departure of the stationary state of the chemical reaction in the plasma from local equilibrium can be quantified using the reaction affinity A_k. There is a reaction affinity for each reaction (R1 and R2). The reaction affinity describes the thermodynamic driving force for the reaction to proceed towards local equilibrium. If the affinity of reaction k is positive then local equilibrium is in the forward direction, if the reaction affinity is negative then local equilibrium is in the reverse direction; and at local equilibrium $A_k = 0$. The reaction affinity of reaction k is defined as:[13]

$$A_k = -\sum_{\text{all species}} \nu_i^k \mu_i, \tag{1}$$

where ν_i^k is the stoichiometric coefficient of species i in reaction k, and μ_i is the chemical potential of species i. Since the sign of the reaction affinity depends on whether there is an accumulation of reactants (positive) or accumulation of products (negative) with respect to the local equilibrium values, the absolute value of A_k can be used to evaluate the magnitude of the departure from local equilibrium to determine if the stationary state is in the nonlinear regime of irreversible thermodynamics. More specifically, if the following criterion is satisfied then the system is in the nonlinear regime:[13]

$$\frac{|A_k|}{RT_b} > 1, \tag{2}$$

where T_b is the background temperature. Criterion (2) can be further understood as describing the departure of the stationary state of the

reaction from local equilibrium. Larger values of $|A_k|/RT_b$ at the stationary state correspond to larger departures from local equilibrium. If the composition at the stationary state is measured after the recombination zone following the plasma, for example, measured from the reactor exhaust, then the magnitude of the reaction affinity at the stationary state calculated using that composition and Equation (1) is an underestimate of what it was at the end of the plasma. Nevertheless, we focus on the reactor exhaust containing metastable molecules because that is the product that could be synthesized by the reactor for later use in an applied context such as biomass or waste plastic processing.

In this experimental work, the effluent composition at long gas residence time in nonequilibrium plasma was measured for the water splitting (R1) and water gas shift (R2) reactions. The effluent composition was measured after the recombination zone. Effluent composition was measured for different feed configurations at the same pressure and plasma generation conditions. More specifically, for the water splitting reaction (R1), a feed composition comprised of a mole fraction of $0.1H_2O$ balance argon was compared to $0.1H_2 + 0.05O_2$ balance argon. For the water gas shift reaction (R2), the feed configurations had mole fractions of $0.1CO + 0.1H_2O$, and $0.1CO_2 + 0.1H_2$. In both cases the balance gas was argon. The stationary states were studied in the pressure range from 2.6 to 21 mbar. Interestingly, it was found that the departure from equilibrium, $|A_k|/RT_b$, for both R1 and R2 was closer to zero at higher pressure. Measurements made using a fluorescence decay temperature probe[14] revealed that the higher-pressure reaction environments produced higher background temperatures. Since the stationary state in the plasma is expected to be relatively insensitive to the background temperature because it is orders of magnitude smaller than the electron temperature,[11] the trend towards local equilibrium with increasing pressure and increasing background temperature is attributed to faster kinetics in the recombination zone. The result suggests a crucial importance of the recombination zone after the plasma in determining the effluent composition, which agrees with previous work.[15] Despite suffering some recombination in the environment governed by local equilibrium following the plasma, very large departures from equilibrium were observed. For example, for Reaction (R1), an influent of $0.1H_2O$ ($|A_1|/RT_b = 0$) was transformed by the plasma into an effluent with approximately 1:1 H_2O:H_2. Departures from local equilibrium for R1, $|A_1|/RT_b$, were observed in the range from 38 to 52. Similarly for Reaction (R2), the effluent was nominally independent of initial speciation. After the recombination zone, Reaction (R2) had a departure from local equilibrium $|A_2|/RT_b$ from 2.8 to 7.2. In both cases, smaller values of $|A_k|/RT_b$ appear at higher pressures and correspondingly higher background temperatures. More interestingly, for both Reactions (R1) and (R2), species accumulated on the endothermic side relative to the equilibrium composition, which is the product side for R1 and the reactant side for R2. For both Reactions (R1) and (R2), the effluent from the reactor, under conditions where the stationary state was reached, was in the nonlinear regime. The results clearly demonstrate that chemical systems involving multiple reactions and multiple species reach stationary compositions in nonequilibrium plasmas that are in the nonlinear regime of irreversible thermodynamics.

2 | METHODS

2.1 | Experimental

The experimental apparatus consisted of a gas delivery manifold, the plasma reactor, and a pumping system including gas composition detection by mass spectroscopy (Figure 1). Gaseous precursors (CO, CO_2, O_2, H_2, and Ar) were delivered with controlled molar flow rates using mass flow controllers (GE50A, MKS Instruments, Andover, MA). The mass flow controllers were calibrated using an absolute standard volumetric flow rate bubble meter (Gilibrator-2, Sensidyne, St. Petersberg, FL). The molar flow rates were calculated using the ideal gas law, which was also used to calculate the total volumetric flow rate through the reactor as a function of the total reactor pressure. Water vapor was delivered by passing an Ar stream through a water bubbler at known temperature (approximately 20°C) and total pressure (approximately 258 mbar). A needle valve was used to control the total pressure in the water bubbler. The water molar flow rate into the reactor was then calculated by doing a steady state mass balance on the bubbler assuming the partial pressure of water in the bubbler effluent was equal to the saturation pressure at the measured temperature. Select experiments were performed to quantify the water molar flow rate using the mass spectrometer, and it was found that the assumption of equilibrium saturation pressure of water was accurate.

The plasma reactor was similar to a previously reported apparatus,[10] with slightly different geometrical dimensions. The total pressure in the reactor was controlled by means of a throttle valve and a vacuum pump. The electrodes were aluminum rings, 1.9 cm ID and 1.3 cm in length separated by a 1.5 cm gap. The inner diameter of the discharge tube was 1.2 cm and the length of the plasma was approximately 4 cm, making for a plasma volume of approximately 4.6 cm^3. The plasma was generated using radiofrequency (RF) excitation at 13.56 MHz using a constant power of 50 W for experiments involving water splitting and 75 W for experiments involving the water gas shift reaction. The generator (AG0613) and matching network (AIT 600) were built by T&C Power conversion (Rochester, NY). Previous research has demonstrated that if the overall atomic fractions of different elements, total pressure, and system geometry are held constant, then the plasma parameters are nominally constant as the total flow rate through the reactor is changed.[10] Double Langmuir probe measurements were previously used to characterize the plasma parameters in similar experiments,[10,14] however, in this work those measurements were found to be unreliable, producing unrealistic electron temperatures of $k_BT_e > 8$ eV. Such erroneously high electron temperatures might be a result of the plasma being electronegative[16] due to the high water content, which is known to form high densities of negative ions.[17] Alternatively, the double Langmuir probe measurements could be erroneous because the electron energy

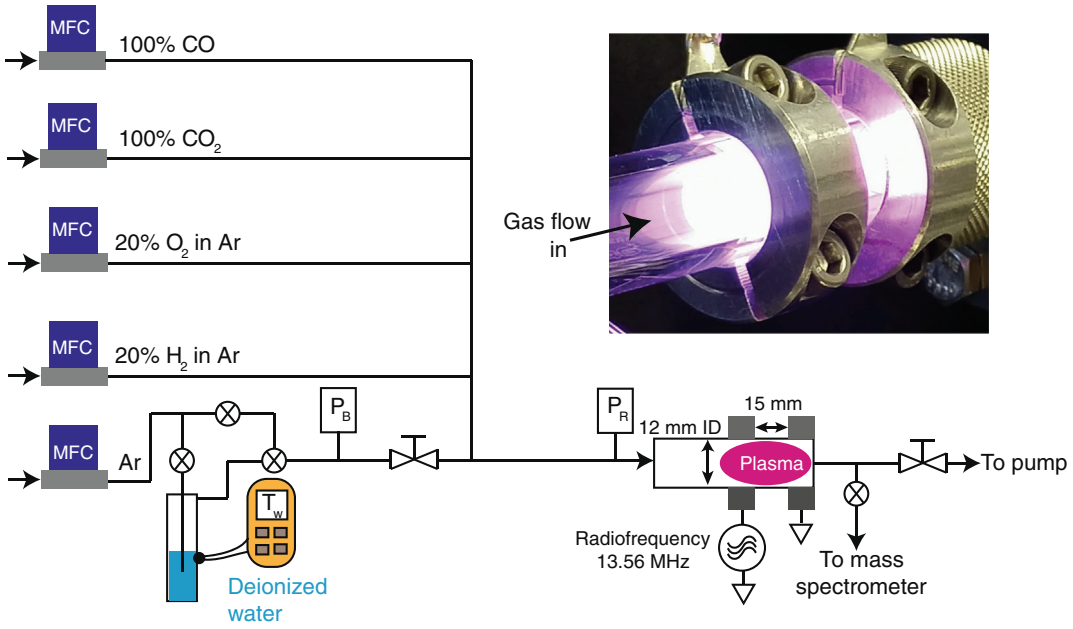

FIGURE 1 Schematic of the experimental apparatus. Symbols are mass flow controller (MFC), water bubbler temperature (T_w) and pressure (P_B), and reactor pressure (P_R). The inset is a digital photograph of the reactor during operation while splitting H_2O into H_2 and $1/2O_2$.

distribution function is non-Maxwellian. As such, the plasma parameters were not measured, but assumed to be constant for a given power, pressure, and overall elemental composition of the gas (either water splitting or water gas shift). The assumption of plasma parameters being constant for constant supplied power density is most reasonable at low total flow rates where the stationary state has been reached in the plasma. If the stationary state has been reached, the overall elemental fractions are the same, and the supplied power density is the same, then the plasma parameters are expected to be nominally independent of the initial speciation (e.g., $0.1H_2O$ vs. $0.1H_2 + 0.05O_2$). Thus, the assumption of constant plasma parameters with constant supplied power density is mainly justified at low total flow rates. The plasma parameters after convergence (vide infra) for water splitting experiments are expected to be similar for the water and hydrogen feed configurations. All water gas shift experiments were conducted at a long residence time where the effluent composition did not depend on whether the reactor was fed carbon monoxide and water, or carbon dioxide and hydrogen. Thus, for long residence times, while the plasma parameters for water splitting and water gas shift experiments were likely different, for a given reaction system, the plasma parameters are expected to be independent of the initial speciation since the volumetric power density was the same. The background gas temperature was estimated by inserting a fluorescence decay probe (Micromaterials Incorporated, Tampa, FL) into the plasma, as previously described.[14]

Gas detection and quantification were done by means of a simple quadrapole mass spectrometer equipped with an electron impact ionizer (XT300, ExTorr Incorporated, New Kensington, PA). The mass spectrometer sensitivity factors were calibrated by measuring gas mixtures of known composition to allow quantification of reactor effluent during plasma reaction. This calibration was performed at each reactor pressure used during experimentation. These calibration factors were found to drift slightly from day-to-day, and thus they were remeasured for every experiment. Mass-to-charge ratios of 2, 18, 28, 32, and 44 were used for H_2, H_2O, CO, O_2, and CO_2 respectively. After all experiments involving feeding H_2O into the reactor, 30 min were allowed to elapse after the bubbler was closed to flush all residual water from the system as observed by the mass spectrometer signal for water returning to the baseline value. After experiments involving synthesizing water by feeding either $H_2 + 1/2O_2$ or $CO_2 + H_2$, 15 min of dry Ar flushing were sufficient to return the 18 AMU peak back to its baseline value. These procedures of flushing residual water from the reactor before moving to the next set of independent variables were found to be crucial to reproducibility.

Water splitting experiments were carried out at a constant reactor pressure of 11 mbar using one of two different feed configurations, which both had the same overall elemental fractions. The feed either had a mole fraction of $0.1H_2O$ balance Ar, or $0.1H_2 + 0.05O_2$ balance Ar. The two feed configurations are termed H_2O and H_2 respectively. For each of these feed configurations, the total flow rate was varied in the range of 50–250 standard cubic centimeters per minute (SCCM) to change the residence time. The residence time was calculated by dividing the reactor volume by the volumetric flow rate, where the volumetric flow rate was calculated using the known molar flow rates and the ideal gas law at the reactor pressure. In this way, the gas residence time in the plasma volume, nominally the portion of the reactor from which light emission was observed, varied from 12 to 60 ms. The average flow velocities that correspond to these residence times were in the range from 0.67 to 3.3 m s^{-1}.

Water gas shift experiments were carried out at a constant total flow rate of 100 SCCM at different pressures in the range from 2.6 to 21 mbar. Two different feed configurations were used that had the same overall elemental fractions. The feed either had a mole fraction of $0.1CO + 0.1H_2O$ balance Ar or $0.1CO_2 + 0.1H_2$ balance Ar. These feed configurations are termed CO and CO_2 respectively. The mass flow controller for CO_2 had a full-scale range of 279 SCCM, and thus the minimum reliable flow rate it could deliver was approximately 10 SCCM. Thus, the total flow rate of 100 SCCM was the smallest value (longest residence time) that was achievable by the experimental apparatus given the pure CO_2 precursor (Figure 1). At all pressures, the residence time at a total flow of 100 SCCM was sufficiently long that the effluent composition was approximately the same for both CO and CO_2 feed configurations.

2.2 | Calculations

Calculation of the reaction affinity for Reactions (R1) and (R2) was done by assuming all species were ideal gasses, which is an excellent assumption at low gas densities like the ones used here, where intermolecular distances are sufficiently large that pairwise potential energy interactions can be neglected and therefore the fugacity coefficient is 1. Assuming ideal gas, the chemical potential of each species can be calculated from the following equation:[13]

$$\mu_i = \mu_i^o(T_b) + RT_b \ln(P_R y_i), \tag{3}$$

where $\mu_i^o(T_b)$ is the standard state free energy of formation of species i at the background temperature T_b, R is the ideal gas constant, P_R is the total reactor pressure in units of bar, and y_i is the mole fraction of species i in the gas phase. Using Equations (1) and (3) together with the stoichiometric relationships R1 and R2, the reaction affinities for the water splitting and water gas shift reactions can be written as a function of the background temperature and mole fractions of different species measured in the effluent:

$$A_1 = -\Delta G_1^o(T_b) + RT_b \ln\left(P_R^{-1/2} \frac{y_{H_2O}}{y_{H_2} y_{O_2}^{1/2}}\right), \tag{4}$$

$$A_2 = -\Delta G_2^o(T_b) + RT_b \ln\left(\frac{y_{CO} y_{H_2O}}{y_{CO_2} y_{H_2}}\right). \tag{5}$$

In Equations (4) and (5), $\Delta G_k^o(T_b)$ is the standard state free energy of reaction for reaction k at the background temperature T_b, which is defined as the sum of the stoichiometric coefficients multiplied by the standard state free energies of formation evaluated at the temperature T_b. The standard state free energies of reaction were estimated as a function of temperature by assuming that the enthalpy of reaction was constant using the van't Hoff equation:

$$\Delta G_k^o(T_b) = \frac{T_b}{298\text{K}} \Delta G_k^o(298\text{K}) + \Delta H_k^o(298\text{K}) \left(1 - \frac{T_b}{298\text{K}}\right), \tag{6}$$

TABLE 1 Thermodynamic information for the water splitting and water gas shift reactions[18]

Species, i	Free energy of formation $\Delta G_i^{of}(298\text{K})$ (kJ mol^{-1})	Enthalpy of formation $\Delta H_i^{of}(298\text{K})$ (kJ mol^{-1})
H_2	0	0
O_2	0	0
H_2O	−228.6	−241.8
CO	−137.2	−110.5
CO_2	−394.4	−393.5
Rxn, k	**$\Delta G_k^o(298\text{K})$ (kJ mol^{-1})**	**$\Delta H_k^o(298\text{K})$ (kJ mol^{-1})**
R1	298.0	241.8
R2	−28.6	−41.2

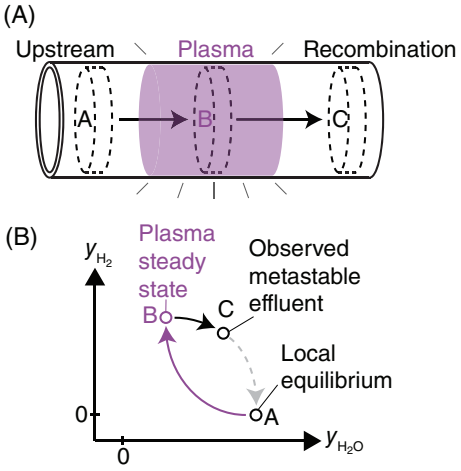

FIGURE 2 Process concept. (A) Schematic of a plug of gas flowing through the plasma and recombination zones. (B) Artistic illustration of composition evolution in the $y_{H_2} - y_{H_2O}$ plane as the gas evolves from the influent composition A, which is at local equilibrium, to the stationary state in the plasma B, and finally recombination to the metastable composition observed by the mass spectrometer C. The observed point C is on the path from the plasma stationary state B to the local equilibrium state A, but the system is kinetically arrested at C and the journey is incomplete, as illustrated by the grayed-out dashed line.

where $\Delta G_k^o(298\text{K})$ and $\Delta H_k^o(298\text{K})$ are the standard state free energy and enthalpy of reaction at 1 bar and 298 K. The reference state information used for Reactions (R1) and (R2) is presented in Table 1.[18]

3 | RESULTS AND DISCUSSION

The key concept is that the plasmachemical reactor has two zones. There is the plasma zone, nominally the volume from which light emission can be observed (Figure 1), and the recombination zone. Consider a plug of gas flowing through a cylindrical tube. The recombination zone is subsequent in space time to the plasma zone (Figure 2A). In

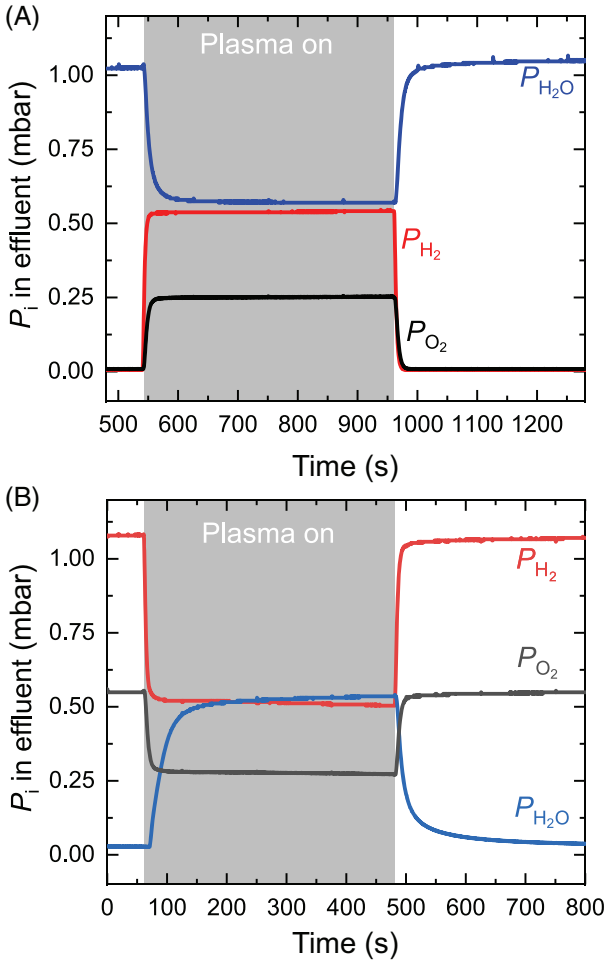

FIGURE 3 Effluent composition for the water splitting reaction (R1) at a residence time of 60 ms at a total pressure of 11 mbar. (A) H_2O feed configuration comprised of a mole fraction of $0.1H_2O$ balance argon. (B) H_2 feed configuration comprised of $0.1H_2 + 0.05O_2$ balance argon. The gray-shaded region is the region where the plasma was on. The blue line is the partial pressure of H_2O as a function of time, the red line is H_2 and the gray line is O_2.

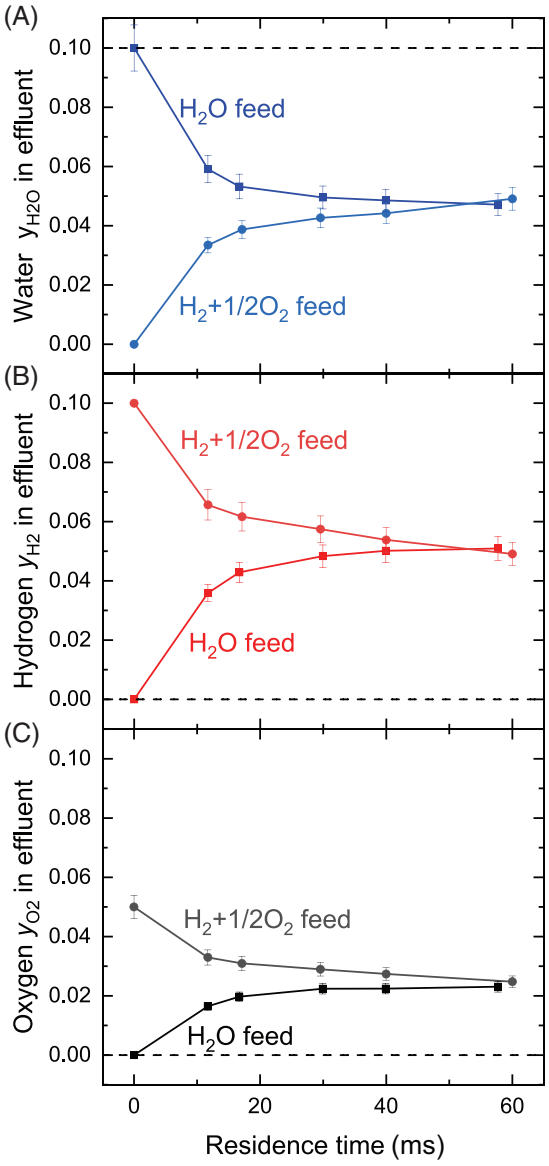

FIGURE 4 Mol fractions of H_2O, H_2, and O_2 as a function of residence time for the water splitting reaction (R1) at a total pressure of 11 mbar. (A) H_2O, (B) H_2, and (C) O_2. The H_2O feed configuration is colored bold and the H_2 feed configuration is muted. The dashed horizontal lines are the equilibrium mole fraction of each species at the background temperature and pressure of the plasma reactor.

these two zones, the chemical reaction proceeds in two fundamentally different directions. In the plasma zone, the reaction proceeds towards a stationary state that is believed to be governed by the principle of maximum entropy production,[11] while in the recombination zone the reaction proceeds towards local equilibrium but typically gets arrested in a metastable state determined by the gas temperature profile and activation barriers (Figure 2B). Since the plasma gets extinguished on a timescale of microseconds,[19] which is much shorter than the gas residence time in the system, the temporal boundary between these two zones is relatively sharp. The composition in the effluent is observed after recombination and therefore depends on the reaction in the plasma zone and the reaction in the recombination zone.

At long residence times in the plasma, the effluent from the reactor in the water splitting experiments did not depend on whether the H_2O or H_2 feed configuration was used. For example, plotted in Figure 3 is the partial pressure of H_2O, H_2, and O_2 as the plasma was turned on and off for a gas residence time of 60 ms in the plasma. The H_2O feed configuration is presented in Figure 3A, and the H_2 feed configuration in Figure 3B. Both feed configurations produced an effluent that was approximately 1:1 H_2:H_2O with a stoichiometric amount of O_2 for Reaction (R1) being the only overall transformation of significance. At significantly shorter residence times, the effluent compositions for the two different feed compositions were not the same. The mole fractions of H_2O, H_2, and O_2 are plotted as a function of residence time for the two different feed configurations in Figure 4A–C respectively. From Figure 4, it can be seen that at a total pressure of 11 mbar and 50 W of applied power, approximately 30–40 ms of residence time were required for the reaction to

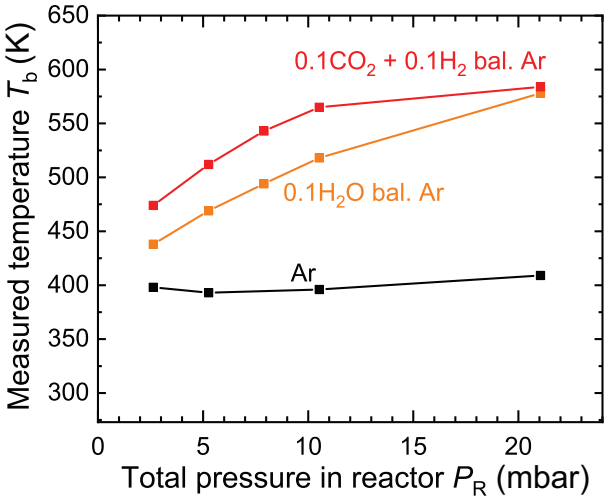

FIGURE 5 Estimated background temperature as a function of total pressure for different gas compositions. RF power was 75 W. Black curve is pure Ar, orange curve is a feed of $0.1H_2O$ balance Ar, and red curve is a feed of $0.1CO_2 + 0.1H_2$ balance Ar.

converge whereafter H_2O and H_2 feed configurations produced the same effluent composition. The time required to reach the stationary state of 30–40 ms is on the same order of magnitude as our previous result in CO_2 splitting at similar total pressure, applied RF power and precursor mole fractions.[10] Moreover, it can be seen from the water feed configuration experiment that the water and hydrogen mole fractions after convergence are dramatically different from their local equilibrium values. Using a background temperature of $T_b = 518$ K (vide infra), the departure from equilibrium of the effluent was $|A_1|/RT_b = 48 \pm 1$ at 60 ms independent of whether a H_2O or H_2 feed configuration was used. The stationary state of the reaction is in the nonlinear regime of irreversible thermodynamics. The energy conversion efficiency was in the range from 1% to 3%, with higher values at smaller water conversions and shorter residence times, as expected.[10] The efficiency is calculated as the molar flow rate of hydrogen in the effluent multiplied by the enthalpy of reaction, divided by the power input as read from the radiofrequency power supply.

For a given applied RF power, the background temperature of the plasma, which can be used to describe the temperature of the neutral and ionized atoms and molecules, depends on the gas composition and total pressure. As the pressure increases, the rate of collisions between hot electrons and neutral molecules increases, and therefore the heat transfer rate to the background gas increases. Furthermore, the gas composition affects the dissipation of hot electron kinetic energy as heat. Heat is transferred to atomic species such as argon by momentum transfer, which is relatively inefficient since the mass of an argon atom is much larger than an electron. Polyatomic molecules can absorb electron energy by vibrational excitation, which has a similar cross-section to momentum transfer but more energy is transferred per collision event.[11] Thus, as the mole fraction of polyatomic molecules in the plasma increases at a given total pressure, the background temperature is also expected to increase as everything else

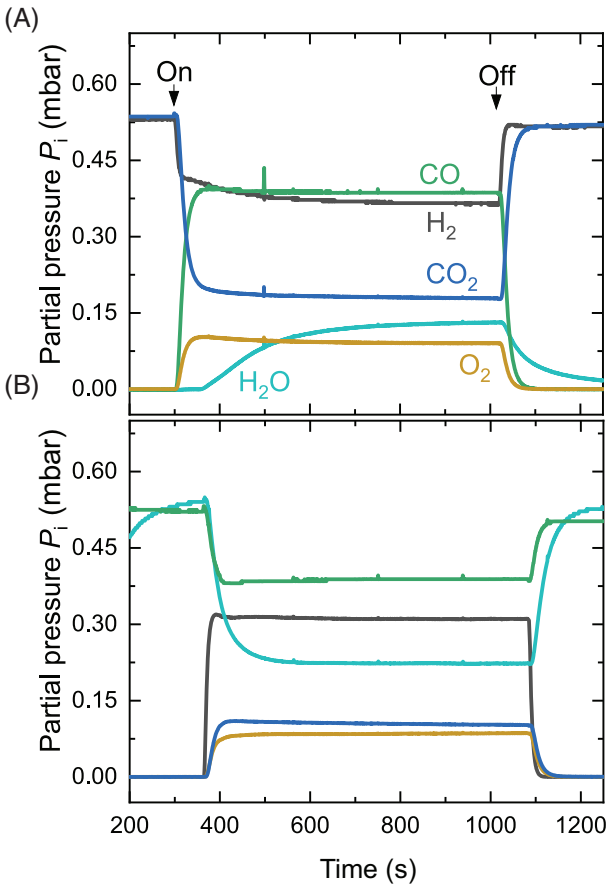

FIGURE 6 Effluent composition for the water gas shift reaction (R2) at a pressure of 5.3 mbar. (A) CO_2 feed configuration comprised of $0.1CO_2 + 0.1H_2$ and (B) CO feed configuration comprised of $0.1CO + 0.1H_2O$. "On" and "Off" indicate where the plasma was turned on and off. The color codes are the same in both panels.

states the same. Ultimately, the background temperature is limited by the power supplied to the plasma and the heat transfer rate to the surrounding environment through the reactor walls.[14] Plotted in Figure 5 is the measured temperature of the fluorescence decay temperature probe inserted into the plasma, which is used here as an estimate of the background temperature, at a constant applied RF power of 75 W. Measurements were made for three different gas compositions: pure Ar, the H_2O feed configuration for R1, and the CO_2 feed configuration for R2. The total flow rate through the system was held constant at 100 SCCM for each curve. All three gas compositions showed increases in temperature with increasing pressure, although the increase was only slight in the case of pure Ar. At all pressures, the presence of molecular gasses increased the background temperature, as expected through the increased heat generation from additional electron kinetic energy loss channels, for example, vibrational excitation of polyatomic molecules followed by vibrational to translational (VT) energy coupling. For pressures less than 20 mbar, at a given pressure, the background temperature increased with the mole fraction of polyatomic molecules in the plasma. In other words, $0.1CO_2 + 0.1H_2$ balance Ar produced a higher background temperature than $0.1H_2O$ balance Ar, which was higher than pure

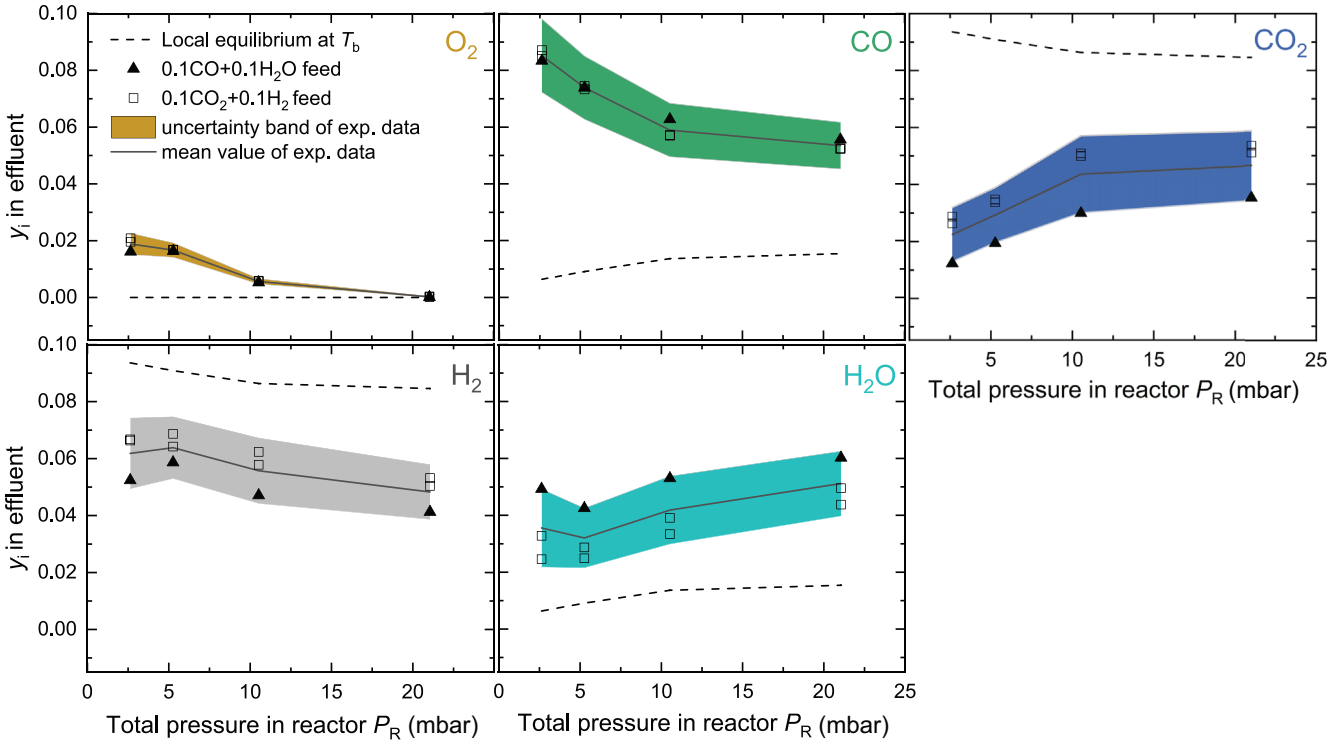

FIGURE 7 Effluent composition for each species at long residence time as a function of total reactor pressure P_R for the water gas shift reaction (R2). The dashed lines indicate the local equilibrium composition at the total pressure and background temperature from Figure 5. The closed symbols are the effluent for the CO feed configuration, and the open symbols are for the CO_2 feed configuration. The shaded region is the uncertainty band of the effluent composition after the recombination zone for the stationary state plasma. The solid line is the mean value of the composition measurements represented by the symbols.

Ar. Qualitatively, it is expected that the rate constant for recombination will be larger at higher pressures in this system since the background temperature is higher.

For the water gas shift reaction (R2), at sufficiently long residence times that the effluent was nominally independent of the feed configuration, the departure from local equilibrium decreased as the pressure increased. The lower limit of the total flow rate our apparatus can supply while maintaining desired influent compositions for water-gas-shift experiments was 100 SCCM, which is just slightly too high to realize robust convergence of the effluent composition starting from both sides of the reaction. The effluent composition for the stationary state in the plasma was determined by averaging measurements made from the two different influent compositions, which resulted in slightly larger uncertainty compared to the water splitting experiments. At a total flow rate of 100 SCCM, at all pressures studied the effluent was approximately the same for the CO_2 ($0.1CO_2 + 0.1H_2$) and CO ($0.1CO + 0.1H_2O$) feed configurations (Figure 6). The partial pressures of the relevant species in the effluent at a total reactor pressure of 5.3 mbar are presented in Figure 6A,B for the CO_2 and CO feed configurations respectively. The only reactions of significance that occurred in this system were Reactions (R1) and (R2). Slight discrepancies were observed for some species at some pressures, suggesting that the flow rate might have been slightly too high to reach robust convergence of the compositions from the different feed configurations, but overall, the shorter residence times at lower pressures were likely compensated for by a higher plasma density and therefore faster kinetics in the plasma zone. Plotted in Figure 7 are the mole fractions of different species in the effluent as a function of pressure for both the CO_2 and CO feed configurations. The mean values of the mole fraction of each species were calculated by averaging the effluent mole fractions determined from the experiments at different feed configurations, and the shaded areas represent the standard deviation of those measurements combined using a root sum of squares with the uncertainty in quantification of species mole fraction using the mass spectrometer. The dashed lines in Figure 7 correspond to the calculated equilibrium mole fraction of each species at the indicated pressure and background temperature from Figure 5. Focusing on the mole fractions of O_2, CO, and CO_2 in Figure 7, as the pressure increased, the mole fractions in the effluent trended towards the equilibrium value at the background temperature and pressure of the reactor. Interestingly, the mole fraction of H_2 and H_2O did not change as much with increasing pressure, and in fact remained very close to the ratio of 1:1 that was observed in the pure water splitting case described above. The most dramatic effect of pressure on effluent composition was with O_2. As total pressure increased, the mole fraction of O_2 in the effluent decreased by two orders of magnitude to just above the detection limit of the apparatus.

The departure of the effluent from local equilibrium can be quantified using the reaction affinity for Reactions (R1) and (R2). Again,

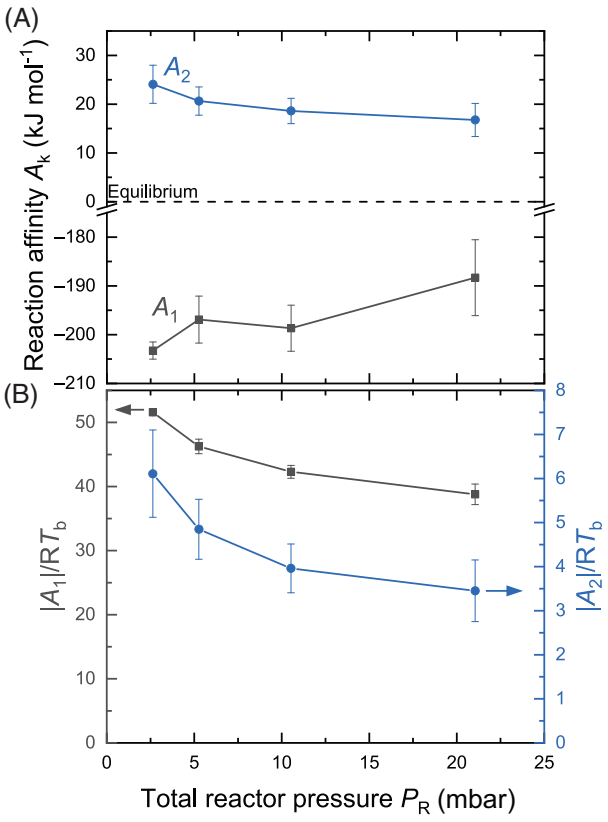

FIGURE 8 Reaction affinities of R1 and R2 for the effluent from the water gas shift experiments as a function of total reactor pressure. (A) Affinity of the water splitting reaction (gray) and water gas shift reaction (blue) for different total reactor pressures. The error bars correspond to the calculated values for repeat experiments at different feed compositions. (B) Departure from local equilibrium in the effluent for Reactions (R1) and (R2) as a function of total reactor pressure. The color codes are the same as (A).

since the temperature increased with reactor pressure at constant applied RF power, and the stationary state in the plasma is expected to have a relatively weak dependence on the background temperature because it is much smaller than the electron temperature,[11] the expectation is that higher pressures will have smaller departures from equilibrium due to faster recombination after the plasma. Plotted in Figure 8A are the reaction affinities A_1 and A_2 calculated using Equations (4)–(6), the background temperature from the red curve in Figure 5, and the measured mole fractions of different species in Figure 7. From Figure 8A, for the endothermic reaction (R1) $A_1 < 0$, meaning products have accumulated relative to their equilibrium mole fractions; while for the exothermic reaction (R2) $A_2 > 0$, meaning reactants have accumulated relative to their equilibrium mole fractions. Therefore, in both cases, the elements accumulated as species in the endothermic direction of Reactions (R1) and (R2). For both reactions, if these species in the effluent were allowed to relax to local equilibrium at the background temperature; heat would be released. Taking the absolute value of the reaction affinity and dividing by RT_b provides the departure from equilibrium as a function of total reactor pressure, which is plotted in Figure 8B. In both cases, $|A_k|/RT_b > 1$, although the departure from local equilibrium decreased as pressure increased, presumably due to faster recombination. On the one hand, we expect that recombination is faster at higher pressures due to elevated background temperature and higher background gas density (Figure 5); however, the evidence presented herein cannot rule out a different stationary state in the plasma. On the other hand, it has been previously argued on theoretical grounds that the background temperature of the plasma plays a negligible role in determining the stationary state in the plasma, provided the electron temperature is much greater than the background gas temperature.[11] Given that the reaction had reached a stationary state in the plasma, as evidenced by the independence of feed composition (Figure 7), and considering the chemistry evolves towards local equilibrium in the recombination zone, the stationary state in the plasma must have been in the nonlinear regime, very far from local equilibrium. In other words, chemical reactions in nonequilibrium plasma evolve towards stationary states in the nonlinear regime of irreversible thermodynamics.

4 | CONCLUSIONS

In conclusion, this work has demonstrated that systems containing multiple reactions and many reactive species (5 in this case) also reach stationary states at long residence times in nonequilibrium plasma. That was demonstrated using the water splitting and water gas shift reactions. The effluent composition was independent of the influent speciation for both the water splitting and water gas shift reactions. In both cases, the species accumulated on the endothermic side of the reaction relative to the local equilibrium values, that is, $H_2 + 1/2O_2$ for water splitting and $CO + H_2O$ for water gas shift. The results suggest that nonequilibrium plasma may be useful for producing hydrogen by water splitting. However, to produce hydrogen from carbon monoxide by water gas shift, thermocatalytic reactors governed by local equilibrium may be more useful to maximize the hydrogen output. The stationary state in the plasma was in the nonlinear regime of irreversible thermodynamics, as evidenced by $|A_k|/RT_b > 1$ observed in the reactor effluent. With increasing pressure, the background temperature of the plasma increased; and also the departure from equilibrium of the gas in the rector effluent decreased. That observation suggests that faster recombination occurs after the plasma when the background gas temperature is higher. The result underscores the critical importance of controlling the recombination zone after the plasma to achieve desired reaction outcomes.

AUTHOR CONTRIBUTIONS

Xiaoshuang Chen: Investigation (equal); methodology (equal); validation (equal); writing – review and editing (equal). **Elijah Thimsen:** Conceptualization (lead); formal analysis (equal); funding acquisition (lead); investigation (equal); methodology (equal); project administration (lead); writing – original draft (lead); writing – review and editing (equal).

ACKNOWLEDGMENT

The authors would like to thank the National Science Foundation for financial support of this work through grant CBET 1847469.

DATA AVAILABILITY STATEMENT

The data that support the findings of this study are available from the corresponding author upon reasonable request.

ORCID

Xiaoshuang Chen https://orcid.org/0000-0002-6324-6417
Elijah Thimsen https://orcid.org/0000-0002-7619-0926

REFERENCES

1. White WB, Johnson SM, Dantzig GB. Chemical equilibrium in complex mixtures. *J Chem Phys*. 1958;28:751-755.
2. Lopez G, Artetxe M, Amutio M, Alvarez J, Bilbao J, Olazar M. Recent advances in the gasification of waste plastics. A critical overview. *Renew Sustain Energy Rev*. 2018;82:576-596.
3. Shahbaz M, Al-Ansari T, Inayat M, Sulaiman SA, Parthasarathy P, McKay G. A critical review on the influence of process parameters in catalytic co-gasification: current performance and challenges for a future prospectus. *Renew Sustain Energy Rev*. 2020;134:110382.
4. Yang H, Fletcher TH, Li Y, et al. Modeling the influence of changes in aliphatic structure on char surface area during coal pyrolysis. *AIChE J*. 2020;66:e16834.
5. Yan B, Cheng Y, Xu P, Cao C, Cheng Y. Generalized model of heat transfer and volatiles evolution inside particles for coal devolatilization. *AIChE J*. 2014;60:2893-2906.
6. Haegel NM, Atwater H, Barnes T, et al. Terawatt-scale photovoltaics: transform global energy. *Science*. 2019;364:836-838.
7. Spitler MT, Modestino MA, Deutsch TG, et al. Practical challenges in the development of photoelectrochemical solar fuels production. *Sustain Energy Fuels*. 2020;4:985-995.
8. DOE. Solar Energy Technologies Office Multi-Year Program Plan (DOE/EE-2346; 8683 2021-05-20). United States 2021.
9. Thimsen E. Beyond equilibrium thermodynamics in the low temperature plasma processor. *J Vac Sci Technol B*. 2018;36:048501.
10. Uner NB, Thimsen E. Superlocal chemical reaction equilibrium in low temperature plasma. *AIChE J*. 2020;66:e16948.
11. Thimsen E. Entropy production and chemical reactions in nonequilibrium plasma. *AIChE J*. 2021;67:e17291.
12. Brown LC, Bell AT. Kinetics of the oxidation of carbon monoxide and the decomposition of carbon dioxide in a radiofrequency electric discharge. II. Theoretical interpretation. *Ind Eng Chem Fundam*. 1974;13:210-218.
13. Kondepudi D, Prigogine I. *Modern Thermodynamics from Heat Engines to Dissipative Structures*. 2nd ed. John Wiley & Sons Inc.; 2015.
14. Uner NB, Thimsen E. Low temperature plasma as a means to transform nanoparticle atomic structure. *Plasma Sources Sci Technol*. 2018;27:074005.
15. Waldo B, Henny B, Bram W, et al. Plasma-driven dissociation of CO_2 for fuel synthesis. *Plasma Processes Polym*. 2017;14:1600126.
16. Amemiya H. Plasmas with negative ions-probe measurements and charge equilibrium. *J Phys D*. 1990;23:999-1014.
17. Nguyen SVT, Foster JE, Gallimore AD. Operating a radio-frequency plasma source on water vapor. *Rev Sci Instrum*. 2009;80:083503.
18. Chase MW Jr. *NIST-JANAF Thermochemical Tables*. 4th ed. American Chemical Society, American Institute of Physics for the National Institute of Standards and Technology; 1998.
19. Husmann E, Thimsen E, Chen X. Particle charge distributions in the effluent of a flow-through atmospheric pressure low temperature plasma. *Plasma Sources Sci Technol*. 2021;30:075030.

How to cite this article: Chen X, Thimsen E. Stationary states of hydrogen-producing reactions in nonequilibrium plasma. *AIChE J*. 2023;69(4):e17952. doi:10.1002/aic.17952